Autophagy restricts fungal accommodation in the roots of *Arabidopsis thaliana*

Patricia Zecua-Ramirez[1], Ernesto LLamas[1,2], Nyasha Charura[1], Nick Dunken[1], Concetta De Quattro[1,2], Alexander Mandel[1], Gregor Langen[1,2] Yasin Dagdas[3], Alga Zuccaro[1,2*]

[1] University of Cologne, Institute for Plant Sciences, Cologne, Germany
[2] Cluster of Excellence on Plant Sciences (CEPLAS), Germany
[3] Gregor Mendel Institute (GMI), Austrian Academy of Sciences, Vienna BioCenter (VBC), Vienna, Austria

* azuccaro@uni-koeln.de

Abstract

Endophytic root colonisation of the host plant *Arabidopsis thaliana* by the beneficial root endophyte *Serendipita indica* is characterised by an initial biotrophic phase followed by a restricted host cell death-associated phase. During colonisation two secreted *S. indica* effectors synergistically produce the cell death inducer deoxyadenosine (dAdo). Although the mechanism of regulated cell death is important for fungal accommodation, the host molecular pathways that restrict *S. indica*-induced cell death and allow the maintenance of a mutualistic relationship are largely unknown. Here we show that autophagy, a major degradation pathway plays a key role in the beneficial interaction between *S. indica* and Arabidopsis. Autophagy restricts fungal colonisation and exerts a protective function against dAdo-induced cell death. Impairment of dAdo uptake in an autophagy mutant background confers resistance to dAdo-induced cell death and precludes the symbiosis-mediated cell death. Taken together, we propose that autophagy-driven pro-survival responses are required to facilitate a long-lasting mutualistic interaction between *S. indica* and Arabidopsis.

Keywords

Arabidopsis thaliana, *Serendipita indica*, endophytic root colonisation, regulated cell death, ATG5, ATG8.

Introduction

Plant-colonising fungi use diverse strategies to interact with their hosts according to their lifestyles (Lo Presti et al., 2015). Beneficial root endophytic fungi of the order Sebacinales (Basidiomycota) establish mutualistic relationships with a variety of plant species (Weiß et al., 2016). Endophytic root associations result in growth promotion as well as enhanced resistance and tolerance against biotic and abiotic stresses (Oberwinkler et al., 2013; Weiß et al., 2016). To colonise plants certain endophytic fungi have evolved mechanisms to counteract the plant immune response, modulate the host metabolism and interfere with its cell death machinery (Deshmukh et al., 2006; Schäfer et al., 2009; Jacobs et al., 2011; Nizam et al., 2019; Dunken et al., 2023).

Root endophytic colonisation of the host plants *Arabidopsis thaliana* (hereafter Arabidopsis) and *Hordeum vulgare* (hereafter barley) by the beneficial fungus *Serendipita indica* (syn. Piriformospora indica) follows a biphasic strategy. *S. indica* establishes an initial biotrophic phase with hyphae enveloped by the host plasma membrane that is followed by a cell death-associated phase (Deshmukh et al., 2006; Qiang et al., 2012; Lahrmann et al., 2013). The induction of host cell death

is restricted to the epidermal and cortex layers of the root and is accompanied by the secretion of hydrolytic fungal enzymes (Zuccaro et al., 2011; Lahrmann and Zuccaro, 2012; Lahrmann et al., 2013, 2015). The induction of this regulated cell death facilitates niche differentiation and ensures nutrient availability, without compromising plant growth (Deshmukh et al., 2006; Zuccaro et al., 2011; Weiß et al., 2016).

Recently, the combined activity of two effectors secreted by *S. indica* during Arabidopsis and barley root colonisation (Thürich et al., 2018; Nizam et al., 2019) was found to produce a DNA-derived deoxynucleoside called deoxyadenosine (dAdo) (Dunken et al., 2023). Extracellular dAdo is imported into the cytoplasm by the Arabidopsis equilibrative nucleoside transporter 3 (ENT3), which functions as a transporter for purine and pyrimidine nucleosides such as adenosine and uridine (Li et al., 2003). dAdo has been described as a cell death inducer in animal systems (Thammavongsa et al., 2013; Winstel et al., 2018). In Arabidopsis, dAdo has been shown to trigger cell death mediated by a nucleotide-binding leucine-rich repeat receptor (NLR) protein with a N-terminal Toll–interleukin-1–receptor (TIR) domain (Dunken et al., 2023). The uptake of dAdo in Arabidopsis also induces the accumulation of metabolites involved in stress signalling and upregulation of cell death marker genes (Olvera-Carrillo et al., 2015; Dunken et al., 2023).

The induction of regulated cell death in host plants by *S. indica* is a crucial process for proper fungal accommodation and symbiosis. However, the host molecular mechanisms that restrict this fungal-induced cell death and allow the maintenance of a mutualistic relationship are largely unknown. We hypothesise that fungal colonisation and the uptake of dAdo trigger a metabolic reprogramming of the host tissue, promoting the activation of pathways aimed at restoring homeostasis and limiting cell death. One potential mechanism that could contribute to the establishment of this beneficial interaction is autophagy, a major degradation and nutrient recycling pathway in eukaryotes. Autophagy is activated by environmental and developmental stimuli and plays a vital role in maintaining cellular homeostasis and modulating metabolism (He and Klionsky, 2009).

Autophagy is known to participate in plant immunity and can either promote or restrict cell death depending on the plant-microbe interaction (Hofius et al., 2017; Üstün et al., 2017; Leary et al., 2019). During biotrophic infections, autophagy regulates the hypersensitive response (HR), which is a localised form of regulated cell death activated by intracellular immune receptors (Jones and Dangl, 2006; Coll et al., 2011). Autophagy components have been shown to promote HR upon infection with avirulent strains, depending on the nature of the immune receptor (Hofius et al., 2009; Hackenberg et al., 2013; Coll et al., 2014; Munch et al., 2015; Han et al., 2015). In non-infected tissue, autophagy plays a protective role by counteracting reactive oxygen species (ROS) production, salicylic acid (SA) signalling, endoplasmic reticulum (ER) stress, and promoting degradation of ubiquitinated proteins, derived from infection-induced systemic responses (Yoshimoto et al., 2009; Munch et al., 2014). During infection with necrotrophic fungi, autophagy promotes resistance and restricts disease-associated lesion formation to the site of infection (Lenz et al., 2011; Lai et al., 2011; Katsiarimpa et al., 2013). Additionally, components of the autophagy machinery participate in mutualistic interactions of *Phaseolus vulgaris* with rhizobacteria and arbuscular mycorrhizal fungi (Estrada-Navarrete et al., 2016).

In animals and plants, autophagy belongs to the protein homeostasis (proteostasis) network and mediates the lysosomal/vacuolar degradation of cytosolic damaged proteins, dysfunctional organelles and protein aggregates. The autophagic cargo is engulfed in double-membrane vesicles called autophagosomes and delivered to the vacuole for breakdown and recycling (He and Klionsky, 2009; Marshall and Vierstra, 2018). Autophagy in plants is broadly divided into microautophagy and macroautophagy (Liu and Bassham, 2012). Macroautophagy (hereafter referred to as autophagy) is mediated by proteins encoded by autophagy-related (ATG) genes. ATG proteins collectively coordinate the biogenesis of autophagosomes (Marshall and Vierstra, 2018). To investigate whether autophagy is involved in *S. indica*-mediated cell death, we use the Arabidopsis knockout (KO) mutants *atg5* and *atg10* that are deficient in autophagosome formation (Thompson et al., 2005; Phillips et al., 2008).

Here we show that autophagy mutants exhibited increased fungal colonisation during the cell death-associated phase, indicating that autophagy restricts colonisation. Live-cell imaging revealed autophagosome formation in the presence of *S. indica*, suggesting the activation of autophagy at the microbe-host interface, as part of a localised defence strategy and metabolic reprogramming. Additionally, autophagy mutants show increased sensitivity to dAdo, and their recovery after dAdo treatment is impaired, indicating that a functional autophagy pathway is essential to recover homeostasis. Furthermore, we demonstrate that impairment of dAdo uptake in the *atg5 ent3* double mutant confers resistance to dAdo-induced cell death and precludes the symbiosis-mediated cell death. Taken together, our results highlight the pro-survival role of autophagy in the beneficial interaction between *S. indica* and Arabidopsis. This suggests that autophagy is a central mechanism for regulating the extent of dAdo-induced cell death, thereby restricting *S. indica* colonisation to maintain a balanced symbiotic interaction.

Results

Autophagy is activated by *S. indica* and restricts fungal colonisation

To determine whether host autophagy is involved in *S. indica* colonisation, we assessed endophytic fungal abundance by quantitative reverse transcription PCR in the Arabidopsis autophagy KO mutants *atg5-3* and *atg10-1* (Fig. 1A). Both autophagy mutants exhibited significantly higher colonisation levels than the Col-0 wild type (WT) at 6 days post-inoculation (dpi), which marks the onset of the cell death-associated phase. This suggests that fungal accommodation is negatively regulated by autophagy. Additionally, we observed an increase in the expression of the ATP and wounding-induced marker gene AT1G58420, which is also responsive to *S. indica* (Choi et al., 2014; Nizam et al., 2019), in colonised roots of autophagy mutants compared to Col-0 at 6 dpi (Fig. 1B). Colonisation of *atg5-3* and *atg10-1* roots also led to an enhanced expression of the immune-related marker genes *WRKY33* and *CYP81F2* compared to Col-0 (Fig. S1), which are involved in the biosynthesis of secondary antimicrobial compounds (Clay et al., 2009; Bednarek et al., 2009; Birkenbihl et al., 2017).

To monitor autophagy activation during *S. indica* colonisation, we used Arabidopsis transgenic lines expressing pUbi::mCherry-ATG8E in WT or in the *atg5-1* KO mutant background. ATG8 is commonly used as a marker to detect and quantify autophagy levels (Yoshimoto et al., 2004; Liu and Bassham, 2012; Klionsky et al., 2021). Confocal microscopy in the differentiation zone of mCherry-ATG8E WT colonised roots revealed an increased amount of mCherry-ATG8E-labelled punctate structures, resembling autophagosomes, compared to mock-inoculated plants (Fig. 1C, E). In contrast, colonised *atg5-1* mutant roots displayed a reduced number of mCherry-ATG8E structures, similar to the larger aggregates previously observed in autophagy-defective mutants (Li et al., 2015) (Fig. 1C, E). We then focused our attention on mCherry-ATG8E WT colonised roots, where we observed that cells in contact with *S. indica* hyphae exhibited an increased number of punctate structures compared to the nearby cells lacking hyphal contact (Fig. 1D, E). These findings provide evidence that *S. indica* induces autophagy at the site of interaction.

We also examined autophagy activation in mock and *S. indica*-colonised mCherry-ATG8E root tissue by immunoblotting. The autophagic turnover of mCherry-ATG8E labelled autophagosomes results in accumulation of the free fluorescent mCherry protein in the vacuole due to faster decay of the ATG8 segment (Chung et al., 2010). Colonisation by *S. indica* led to an increased proportion of free mCherry compared to mock treatment, confirming induction of autophagic activity by the fungus (Fig. 1F). Interestingly, we detected an additional mCherry-ATG8E cleavage fragment produced in both WT and mutant background in the presence of *S. indica*, independent from the *atg5-1* mutation. This additional fragment is not produced upon autophagy induction due to carbon starvation (Fig. 1F). These findings suggest that, in addition to the induction of autophagy, *S. indica* colonisation triggers an ATG5-independent hydrolysis of ATG8. Furthermore, we analysed transcriptomic data from Arabidopsis roots colonised by *S. indica* at different time

points. We observed an induction in the expression of autophagy-associated genes including the autophagy-related genes (ATGs) of the core autophagy machinery (Mizushima et al., 2011; Liu and Bassham, 2012) (Fig. 1G, S2). Taken together, these results demonstrate that autophagy is activated during *S. indica* colonisation.

Autophagy promotes cell survival during dAdo-induced cell death

During the cell death-associated phase of *S. indica* colonisation, two fungal apoplastic effector enzymes produce extracellular dAdo. dAdo induces cell death in various plant species, including Arabidopsis (Dunken et al., 2023). Since autophagy plays a role in promoting cell survival and maintenance of cellular homeostasis, we investigated whether it could restrict dAdo-induced cell death. To test this hypothesis, we measured the onset of cell death by monitoring the photosynthetic efficiency, which reflects the health status of the plant and decreases under biotic, abiotic stress or cell death (Dunken et al., 2022). Our results showed that treatment with dAdo strongly decreased the maximum quantum yield of photosystem II (F_V/F_M) in *atg5-3* and *atg10-1* KO mutants compared to Col-0 (Fig. 2A, C and S3). Similar enhanced sensitivity was observed during seed germination tests with *atg5-3* mutants upon treatment with dAdo (Fig. S4). To confirm the functionality of the autophagy mutants, we also assessed their sensitivity to methyl jasmonate (MeJA), a senescence inducer, as a positive control (He et al., 2002). The results showed that autophagy mutants exhibited increased sensitivity to MeJA (Fig. 2B, C and S3). We further investigated the role of autophagy by testing other mutants involved in the formation and expansion of autophagosomes. Treatment with dAdo affected the germination of *atg2-2* and induced a significant reduction in the photosynthetic efficiency of *atg11-1* compared to Col-0 (Fig. S3, S5). These results demonstrate that autophagy mutants show increased sensitivity to dAdo, further supporting the role of autophagy in response to stress and cell death.

To study the protective role of autophagy in more detail, we tested the ability of autophagy mutants to recover after dAdo and MeJA treatment by monitoring the photosynthetic efficiency. We removed the treatments by exchanging dAdo and MeJA treatment solutions with buffer at 24 h post-treatment. Interestingly, while Col-0 seedlings were able to recover, the autophagy *atg5-3* and *atg10-1* mutants showed an irreversible induction of cell death under treatment with both dAdo (Fig. 2D, F) and MeJA (Fig. 2E, F). These observations highlight that when autophagy is impaired, dAdo leads to an enhanced and irreversible induction of cell death at early time points. Notably, we observed that recovery was impaired in Col-0 seedlings after 48 h of treatment (Fig. S6), suggesting the occurrence of a point-of-no-return during the execution of dAdo-induced cell death. Collectively, these results support the notion that autophagy exerts a detoxifying function against cellular stress induced by dAdo.

dAdo sensitivity in *atg5* mutant plants is dependent on uptake

The import of extracellular dAdo by the ENT3 transporter is required for dAdo-dependent regulated cell death (Dunken et al., 2023). We hypothesised that impaired dAdo uptake in *atg5-3* mutant plants would generate dAdo resistance, thereby reducing cell death. To test this effect, we generated an *atg5 ent3* double mutant. Examination of the photosynthetic efficiency in seedlings incubated with mock or dAdo showed that the double mutant gained resistance to dAdo, similar to the *ent3* mutant, exhibiting reduced sensitivity (Fig. 3A). The double mutant exhibited increased sensitivity to MeJA, indicating that mutation of the ENT3 transporter confers a specific resistance phenotype to the cell death trigger dAdo but not to MeJA (Fig. 3B). To evaluate the extent of cell death we used the Evans blue dye, which selectively permeates through cells with ruptured plasma membranes. Quantification of cell death after mock or dAdo treatment was performed using bright-field microscopy. After a 4-day dAdo treatment, we observed stained dead cells primarily at the root tip compared to the mock control, confirming cell death (Fig. 3C, D). The *atg5-3* autophagy mutant displayed enhanced cell death, while impairment of the ENT3 transporter limited its extent compared to Col-0. Notably, the *atg5 ent3* double mutant exhibited

an intermediate dAdo-sensitive phenotype between *atg5-3* and *ent3* (Fig. 3C, D). These findings indicate that impaired dAdo uptake in *atg5 ent3* mutant plants leads to reduced cell death and increased resistance to dAdo.

S. indica-mediated cell death is supported by the production of dAdo (Dunken et al., 2023). To assess the impact of reduced sensitivity to dAdo in the *atg5 ent3* double mutant on root colonisation, we performed colonisation assays on half strength MS media and evaluated cell death using Evans blue dye at 12 dpi. While *S. indica* colonisation induced cell death in the differentiation zone of Col-0 and the *atg5-3* single mutant compared to mock conditions, the *atg5 ent3* double mutant showed no significant differences in cell death between *S. indica* and mock treatments, indicating that the double mutation precludes the symbiosis-mediated cell death (Fig. 4A, B). Assessment of endophytic fungal abundance revealed higher colonisation levels in both *atg5-3* and *atg5 ent3* double mutant lines compared to Col-0 (Fig. 4C). These findings correlate with increased levels of dead cells in both *atg5-3* and *atg5 ent3* lines under mock conditions in the root differentiation zone, when compared to Col-0 control (Fig. 4A, B).

To investigate the involvement of autophagy in *S. indica*-mediated growth promotion, we quantified the root length of colonised seedlings after 21 days. Colonisation was performed on minimal medium (1/10 PNM), which enhances the beneficial effects of the root endophyte on host plants. *S. indica* treatment of Col-0 resulted in longer primary roots compared to mock conditions, indicating that *S. indica*-induced cell death does not affect the fungal-mediated root growth phenotype (Fig. 4D). Fungal-inoculated *atg5* mutants showed no increase in root growth compared to the mock control (Fig. 4D), suggesting that the lack of autophagy affects the root growth phenotype induced by *S. indica*. Taken together, our results support the role of autophagy as a survival mechanism to reduce dAdo-induced cell death, thereby restricting *S. indica* colonisation and maintaining a balanced interaction (Fig. 5).

Discussion

Our investigation into the interaction between the plant host Arabidopsis and the endophytic fungus *S. indica* has shed light on the role of autophagy in restricting fungal colonisation. Our results demonstrate that loss of function of ATG5 and ATG10 leads to increased colonisation by the fungus, especially during the cell death-associated phase (Fig. 1A, 4C). Additionally, we analysed the transcriptional response to *S. indica* in autophagy mutant roots. Expression of the *S. indica*-responsive marker gene AT1G58420 is increased in the mutants compared to Col-0, which correlates with an increase in fungal biomass. Moreover, the upregulation of two additional marker genes, *CYP81F2* and *WRKY33*, further supported this observation. The WRKY33 transcription factor is known to target genes like *CYP81F2* involved in the production of secondary metabolites, such as glucosinolates, and the regulation of plant hormone pathways (Birkenbihl et al., 2017). These findings suggest that autophagy may contribute to the plant immune response, as evidenced by the interaction between WRKY33 and ATG18a during necrotrophic infections in Arabidopsis (Lai et al., 2011). Furthermore, analysis of the transcriptional response of Arabidopsis genes associated with the autophagy core process and its regulation highlights the importance of autophagy, particularly during later stages of colonisation by *S. indica* (Fig. 1G, S2).

To confirm autophagy activation in *S. indica*-colonised root cells, we examined autophagosome formation using mCherry-ATG8E transgenic lines. Our results showed the presence of autophagosome-resembling structures in colonised and to a lesser extent in neighbouring cells, but not in the *atg5-1* mutant background line (Fig. 1C-E). The occurrence of autophagosomes during selective autophagy at the host-microbe interface has been reported as part of the localised immune response (Dagdas et al., 2018; Pandey et al., 2021). Selective autophagy has also been reported to alleviate ER stress, which is known to arise during the *S. indica* cell death-associated phase (Qiang et al., 2012), by facilitating the removal of certain ER domains (Stephani et al., 2020). Local autophagy activation may also coordinate the metabolic reprogramming during *S. indica* colonisation. In barley, *S. indica*-induced resistance to fungal diseases and salt stress is associated with an enhanced antioxidant capacity (Waller et al., 2005). Additionally, *S. indica* influences transcriptional responses and metabolite profiles by regulating the expression of genes involved in hormonal signalling pathways (e.g., salicylic acid, jasmonic acid, ethylene, and auxin) and causing changes in amino acid concentrations during colonisation (Schäfer et al., 2009; Lahrmann et al., 2013). Therefore, autophagy may serve as a mechanism controlling the reprogramming of hormonal signalling or the reallocation of nutrients.

Moreover, immunoblot analysis showed increased mCherry-ATG8E cleavage, indicating higher autophagic flux during fungal colonisation. The observed mCherry-ATG8E cleavage pattern in the *S. indica* colonised *atg5-1* line (Fig. 1F) suggests the involvement of an independent mechanism of hydrolysis in addition to ATG5-dependent autophagy. This effect can be attributed to the hydrolytic activity occurring during the cell death-associated phase, where plant lytic enzymes, including proteases, may contribute to the degradation process. Additionally, this colonisation stage is characterised by the release of numerous fungal proteases and cell wall modifying enzymes (Zuccaro et al., 2011; Lahrmann and Zuccaro, 2012; Lahrmann et al., 2015). However, it cannot be ruled out that other degradation mechanisms may be activated in the presence of the fungus when the autophagic pathway is non-functional. One potential mechanism is the ubiquitin-proteasome system, which has been reported to have crosstalk with autophagy (Raffeiner et al., 2023).

Autophagy is a degradation pathway that promotes a protective response to stress situations. For instance, autophagy prevents the precocious onset of senescence and facilitates nutrient remobilisation during senescence (Schippers et al., 2007). Treatment with MeJA led to accelerated senescence-associated cell death in the autophagy mutants (Fig. 2B, C), resembling the early senescence phenotype previously described for different autophagy mutants including *atg5* and *atg10* (Doelling et al., 2002; Hanaoka et al., 2002; Thompson et al., 2005; Phillips et al., 2008; Yoshimoto et al., 2009). We also demonstrate autophagy involvement during dAdo-induced cell

death, as evidenced by the increased sensitivity of *atg5-3*, *atg10-1*, *atg2-2* and *atg11-1* mutants to dAdo and reduced sensitivity in the *atg5 ent3* double mutant having a non-functional nucleoside transporter (Fig. 2A, 3A, S4, S5). Furthermore, *atg5-3* and *atg10-1* mutants displayed impaired recovery compared to Col-0 after dAdo treatment (Fig. 2D, F) highlighting the pro-survival function of autophagy.

dAdo induces cell death and various metabolic alterations such as the expression of cell death marker genes, electrolyte leakage, activation of the 26S proteasome and extracellular accumulation of the retrograde stress signalling metabolite methylerythritol cyclodiphosphate (MEcPP) (Dunken et al., 2023). The homeostatic functions observed during senescence and other stress conditions may be similar to the autophagic responses that potentially counteract the effects of dAdo. These cytoprotective functions include the degradation of protein aggregates and damaged organelles for recycling (Xiong et al., 2007; Wada et al., 2009; Munch et al., 2014). Autophagy can also participate in the degradation of pro-death signals (Hayward et al., 2009) and regulate proteostasis by selectively degrading inactive proteasomes via the proteasome subunit RPN10 (Marshall et al., 2015). Together, these responses also suggest that autophagy may serve as a molecular checkpoint to mediate between cell death and metabolism, as proposed in the animal field (Green et al., 2014).

The fungal-induced cell death involves the production of dAdo and the uptake by the ENT3 transporter (Dunken et al., 2023). As a result, the *ent3* mutant line did not display altered cell death in the presence of the fungus compared to mock conditions at 12 dpi (Fig. 4A). Similarly, the colonised *atg5 ent3* double mutant also showed no fungal-induced cell death, reflecting the *ent3* phenotype in the context of cell death (Fig. 4A). However, during fungal colonisation, the double mutant demonstrated a phenotype resembling the *atg5-3* mutant that exhibited increased colonisation levels (Fig. 4C). This divergence in phenotype can be attributed to an additional form of cell death occurring in the autophagy mutants independent of *S. indica* colonisation. This susceptibility to cell death is thought to be due to the loss of homeostatic functions in autophagy-deficient plants, which, in turn, supports colonisation by the root endophyte. *S. indica* is a symbiont with inherent saprotrophic properties that benefits from a nutritional strategy through the degradation of dead root material after an initial biotrophic phase. This is consistent with the upregulation of transcripts encoding genes involved in protein hydrolysis and transport during the transition from biotrophy to the cell death-associated phase, as shown by transcriptome analyses (Zuccaro et al., 2011) and genomic analyses of the Serendipitaceae which display biotrophic and saprotrophic features (Lahrmann and Zuccaro, 2012; Oberwinkler et al., 2013).

The sensitised state in the *atg5* mutant is amplified by the loss of function of the nucleoside transporter ENT3 in the double mutant (Fig. 4A). In plants and mammals, depletion of cellular purine nucleotides levels has been shown to trigger the activation of autophagy by inhibiting TOR (Target of Rapamycin), a key regulator of growth and a nutrient sensor that negatively regulates autophagy (Hoxhaj et al., 2017; Kazibwe et al., 2020). Additionally, AtENT3 has been proposed to participate in the salvage pathway of nucleotide synthesis (Li et al., 2003). Therefore, an alteration in the nucleotide pool resulting from a double metabolic deficiency may lead to increased cellular stress in the double mutant.

We also examined Arabidopsis root growth and observed that under nutrient-limiting conditions, Col-0 exhibited longer primary roots in the presence of *S. indica* compared to the mock condition (Fig. 4D). However, this phenotype was not observed in the *atg5* autophagy mutant, suggesting that autophagy can influence the fungal-mediated root growth phenotype induced by the fungus under nutrient-limiting conditions. These findings highlight the importance of nutrition for future research in understanding this mutualistic relationship.

Our experiments show that autophagy activation is involved in fungal growth restriction and is required to promote cell survival during dAdo-induced cell death. We propose that the activation of autophagy and likely other proteostasis mechanisms in colonised cells, promotes a protective response to restrict fungal-induced stress and cell death, maintaining a balanced

symbiotic interaction (Fig. 5). These results also demonstrate the complexity of the *S. indica* colonisation process, in which nutritional factors, metabolic status and immune-related cell death are modulated by autophagy and influence the extent of fungus-induced cell death.

Materials and Methods

Plant lines

Arabidopsis thaliana ecotype Columbia (Col-0) was used as a wild-type control. The T-DNA insertion mutant lines in this study are: *atg5-1* (AT5G17290) SAIL-129B07, *atg5-3* SALK-020601C (Thompson et al., 2005; Havé et al., 2019), *atg10-1* (AT3G07525) SALK-084434, *atg11-1* (AT4G30790) SAIL-1166G10, *atg2-2* (AT3G19190) EMS-mutant (Gln803stop) (Wang et al., 2011), *ent3* (AT4G05120) SALK-204257C. The transgenic lines pUbi::mCherry-ATG8E in Col-0 WT and *atg5-1* background (Stephani et al., 2020). The double mutant *atg5 ent3* was obtained by crossing *atg5-3* and *ent3* lines. All transgenic lines were genotyped by PCR and homozygous lines were isolated.

Plant-growth conditions

Surface-sterilised seeds of Arabidopsis were germinated and grown on ½ MS (Murashige-Skoog Medium, with vitamins, pH 5.7) containing 0.5%(w/v) sucrose and 0.4% (w/v) Gelrite (Duchefa, Haarlem, the Netherlands) and stratified in darkness for 3 days at 4°C. Plants were grown under short day conditions (8 h light, 16 h dark) with 130 µmol m^{-2} s^{-1} of light and 22°C/18°C.

Fungal strains and culturing techniques

Serendipita indica strain DSM11827 (German Collection of Microorganisms and Cell Cultures) Braunschweig, Germany) was grown on complete medium (CM) containing 2% (w/v) glucose and 1.5% (w/v) agar at 28°C as described (Hilbert et al., 2012). For confocal microscopy studies, the *S. indica* strain constitutively expressing a *S. indica* codon-optimised GFP gene was used (Hilbert et al., 2012).

Fungal inoculation

Eight-day-old Arabidopsis seedlings were transferred to ½ MS (Murashige-Skoog Medium, with vitamins, pH 5.7) and 0.4% (w/v) Gelrite plates. Nine-day-old seedlings and surrounding area were inoculated with 800 µL containing $5*10^5$ *S. indica* chlamydospores / mL. Control plants were inoculated with sterile milli-Q water as mock. At the indicated time points, a 4 cm root section was harvested starting 0.5 cm below the shoot. The material was washed thoroughly and frozen in liquid nitrogen. Each biological replicate contains three plates with 15 seedlings each. For seed inoculation, surface-sterilised Arabidopsis seeds were incubated in 600 µL containing $5*10^5$ *S. indica* chlamydospores / mL or sterile milli-Q water for 1 hour followed by their distribution on ½ MS and 0.4% (w/v) Gelrite plates.

RNA extraction and real-time quantitative PCR analysis

Total RNA was extracted from colonised or mock-treated ground plant root material using TRIzol reagent (Invitrogen, Thermo Fisher Scientific, Schwerte, Germany) according to the manufacturer's instructions and digested with DNase I to prevent genomic DNA contamination (Thermo Fisher Scientific, Schwerte, Germany). cDNA was synthesised with 1 µg total RNA primed with Oligo-dT and random hexamers primers using the First Strand cDNA Synthesis Kit (Thermo Fisher Scientific, Schwerte, Germany). Quantitative real-time PCR was performed using the 2x GoTaq qPCR master mix (Promega, Walldorf, Germany) with 10 ng of cDNA template and 0.5 µM of each oligonucleotide in a final volume of 15 µL. Reactions were amplified in a CFX connect real time system (BioRad, Munich, Germany) according to the following protocol 95°C 3

min, 95°C 15 s, 59°C 20 s, 72°C 30 s, 40 cycles and a melting curve analysis. Relative expression was calculated using the $2^{-\Delta C_t}$ or $2^{-\Delta\Delta C_t}$ method. Sequences of all primers can be found in Table S1.

PAM fluorometric measurements

For chlorophyll fluorescence analysis, eight-day-old Arabidopsis seedlings were transferred to 24-well plates (three per well) containing 2 mL of 2.5 mM MES buffer (pH 5.6). After overnight regeneration, seedlings were treated with mock (MES 2.5 mM buffer), dAdo or methyl jasmonate (Sigma-Aldrich, Taufkirchen, Germany) to a final concentration of 500 µM. Maximum quantum yield of photosystem (PS)-II (F_V/F_M) of dark-adapted samples was quantified using Pulse Amplitude Modulation (PAM) fluorometry (M-Series PAM fluorometer, Heinz Walz GmbH, Effeltrich, Germany). Data were analysed using ImagingWin software (V2.56p; Walz, Germany).

Seed germination assays

Surface-sterilised seeds of Arabidopsis were transferred to 24 well plates, containing 2 mL of 1/10 PNM (Plant Nutrition Medium, pH 5.7). The medium was supplemented with 500 µM dAdo or mock (2.5 mM MES, pH 5.6). 10 seeds were placed into each well and after 2 days of stratification, grown under short day conditions. The growth of the seedlings was monitored via PAM fluorometry at 8, 14 and 21 days after transfer to the growth chamber. Analysis of the photosynthetic active area was analysed using the software Fiji (ImageJ).

Root length measurements

Surface-sterilised Arabidopsis seeds were inoculated with mock or *S. indica* spores on plates containing 1/10 PNM (Plant Nutrition Medium, pH 5.7). 21 days after inoculation, scans of the square plates containing seedlings were taken. Images were analysed using Fiji (ImageJ) to measure the length of the primary root (cm) of seedlings developing true leaves.

Cell death staining with Evans Blue

Root cell death was quantified using Evans blue dye (Sigma-Aldrich, Taufkirchen, Germany) to assess *S. indica*- or dAdo-induced cell death at the indicated time points. Treated roots were washed three times with milli-Q water before staining with 2.5 mM Evans blue solution in 0.1 M $CaCl_2$ pH 5.6 for 15 min. After 1 hour of washing, root images were taken using a Leica M165 FC stereo microscope. The microscopy of *S. indica* colonised samples was performed using the differentiation zone of the Arabidopsis roots, and the microscopy of the roots treated with dAdo corresponds to the root tip. Quantification of cell death was performed using Fiji (ImageJ).

Autophagic flux assay

For carbon starvation treatment, Arabidopsis seedlings expressing pUbi::mCherry-ATG8E in WT or in the *atg5-1* KO mutant background were grown on ½ MS containing 1% (w/v) sucrose and 0.4% (w/v) Gelrite. After 7 days, seedlings were transferred to ½ MS without sucrose and plates were covered with aluminium foil and grown under the same conditions for 9 days (Stephani et al., 2020). Whole seedlings were harvested and frozen in liquid nitrogen.

For analysis during *S. indica* colonisation, surface-sterilised Arabidopsis seeds were inoculated with mock or *S. indica*. After 10 days, root tissue was harvested and frozen in liquid nitrogen.

Protein extraction and immunoblot analysis

Frozen samples were homogenised with a bead mill (TissueLyser II, Qiagen) for 2 min (frequency 30^{-1}). 1x lysis buffer (300 mM NaCl, 100 mM HEPES pH 7.4, 2 mM EDTA, 2% Triton X-100)

with 1x plant protease inhibitor cocktail (Sigma-Aldrich, Taufkirchen, Germany) and 1 mM PMSF was added and samples were vortexed. The lysates were cleared by centrifugation at 13,000 g for 10 min at 4°C. Protein concentration was determined using the Pierce BCA Protein Assay Kit (Thermo Fisher Scientific, Schwerte, Germany). SDS-PAGE was performed with 10% gels and 1x Tris Glycine-SDS buffer (BioRad, Munich, Germany). Semi-dry blotting was performed on PVDF membranes. Membranes were blocked with 3% BSA (VWR, Darmstadt, Germany) in TBS and 0.05% Tween 20% (v/v) (TBS-T) for 1 hour at room temperature. After incubation overnight at 4°C with the primary antibody anti-mCherry (1:1000, 5993, BioVision) diluted in 1x phosphate-buffered saline (PBS), the membranes were washed three times with TBS-T. After a 40 min incubation with the secondary antibody IRDye 800CW (1:10,000, LI-COR) diluted in 3% BSA TBS-T, the membranes were washed three times with TBS-T and finally rinsed with 1x PBS. Fluorescent Western blot detection was performed using an Odissey DLx (LI-COR Biosciences GmbH, Bad Homburg vor der Höhe, Germany).

Confocal imaging and image quantification

A TCS SP8 confocal microscope (Leica, Wetzlar, Germany) was used for confocal laser scanning microscopy on living cells. mCherry was excited by a laser light at 561 nm and the emitted light was detected with a hybrid detector (HyD2) at 602-638 nm. The mCherry-ATG8-labelled punctate were counted in a 63x captured image size (184.52 µm x 184.52 µm) considering maximal projections of 8-10 frames with 4 µm step size.

Statistical analysis

Analysis was performed using GraphPad Prism software (v.9.4.1 for Windows) or RStudio (R v.4.1.1 for Windows). The detailed statistical method is given in the figure legends.

Transcriptomic analysis (RNA sequencing)

Arabidopsis Col-0 WT roots were inoculated with mock (milli-Q water) or *S. indica*. Roots were harvested at 1, 3, 6, and 10 days post-inoculation. For each condition three biological replicates were considered. For each sample, stranded RNA-Seq libraries were generated and quantified by qPCR. The RNA-Seq libraries were generated and sequenced at US Department of Energy Joint Genome Institute (JGI) under a project proposal (Proposal ID: 505829) (Zuccaro & Langen, 2020). The raw reads were filtered and trimmed using the JGI QC pipeline. Filtered reads from each library were aligned to the Arabidopsis (TAIR10) reference genome using HISAT2 (Kim et al., 2015) and the gene counts were generated using featureCounts (Liao et al., 2014). DESeq2 was used to perform differential gene expression analysis (Love et al., 2014). Autophagy-associated genes were identified using the Gene ontology (GO) terms annotated by Denny et al. (2018) and retrieved from the Arabidopsis (TAIR10) annotation version 2023-05-01.

Acknowledgments

We would like to thank Prof. Ralph Hückelhoven for providing constructive feedback and Martin Stegmann for critical reading of the manuscript. We would like to thank Lisa Mahdi for conducting experiments for the RNA-seq analysis. We extend our gratitude to the U.S. Department of Energy, Joint Genome Institute (https://ror.org/04xm1d337) and Yu Zhang, Sravanthi Tejomurthula, Daniel Peterson, Vivian Ng & Igor Grigoriev for producing sequencing data within the work proposal 10.46936/10.25585/60001292.

Funding

German Research Foundation (DFG), SFB 1403- Cell Death in Immunity, Inflammation and Disease- Project ID: 1403-414786233 (PZ, ND, AZ).
German Research Foundation (DFG), Excellence Strategy, Cluster of Excellence on Plant Sciences (CEPLAS) - EXC-2048/1 - Project ID 390686111 (EL, NC, CDQ, AZ).

References

P. Bednarek, M. Pislewska-Bednarek, A. Svatos, B. Schneider, J. Doubsky, M. Mansurova, M. Humphry, C. Consonni, R. Panstruga, A. Sanchez-Vallet, A. Molina, and P. Schulze-Lefert. A glucosinolate metabolism pathway in living plant cells mediates broad-spectrum antifungal defense. *Science*, 323(5910):101–106, 2009. doi: 10.1126/science.1163732.

R. P. Birkenbihl, B. Kracher, M. Roccaro, and I. E. Somssich. Induced genome-wide binding of three arabidopsis wrky transcription factors during early mamp-triggered immunity. *The Plant cell*, 29(1):20–38, 2017. doi: 10.1105/tpc.16.00681.

J. Choi, K. Tanaka, Y. Cao, Y. Qi, J. Qiu, Y. Liang, S. Y. Lee, and G. Stacey. Identification of a plant receptor for extracellular atp. *Science*, 343(6168):290–294, 2014. doi: 10.1126/science.343.6168.290.

T. Chung, A. R. Phillips, and R. D. Vierstra. Atg8 lipidation and atg8-mediated autophagy in arabidopsis require atg12 expressed from the differentially controlled atg12a and atg12b loci. *The Plant journal : for cell and molecular biology*, 62(3):483–493, 2010. doi: 10.1111/j.1365-313X.2010.04166.x.

N. K. Clay, A. M. Adio, C. Denoux, G. Jander, and F. M. Ausubel. Glucosinolate metabolites required for an arabidopsis innate immune response. *Science*, 323(5910):95–101, 2009. doi: 10.1126/science.1164627.

N. S. Coll, P. Epple, and J. L. Dangl. Programmed cell death in the plant immune system. *Cell death and differentiation*, 18(8):1247–1256, 2011. doi: 10.1038/cdd.2011.37.

N. S. Coll, A. Smidler, M. Puigvert, C. Popa, M. Valls, and J. L. Dangl. The plant metacaspase atmc1 in pathogen-triggered programmed cell death and aging: functional linkage with autophagy. *Cell death and differentiation*, 21(9):1399–1408, 2014. doi: 10.1038/cdd.2014.50.

Y. F. Dagdas, P. Pandey, Y. Tumtas, N. Sanguankiattichai, K. Belhaj, C. Duggan, A. Y. Leary, M. E. Segretin, M. P. Contreras, Z. Savage, V. S. Khandare, S. Kamoun, and T. O. Bozkurt. Host autophagy machinery is diverted to the pathogen interface to mediate focal defense responses against the irish potato famine pathogen. *eLife*, 7, 2018. doi: 10.7554/eLife.37476.

P. Denny, M. Feuermann, D. P. Hill, R. C. Lovering, H. Plun-Favreau, and P. Roncaglia. Exploring autophagy with gene ontology. *Autophagy*, 14(3):419–436, 2018. doi: 10.1080/15548627.2017.1415189.

S. Deshmukh, R. Hückelhoven, P. Schäfer, J. Imani, M. Sharma, M. Weiss, F. Waller, and K.-H. Kogel. The root endophytic fungus piriformospora indica requires host cell death for proliferation during mutualistic symbiosis with barley. *Proceedings of the National Academy of Sciences*, 103(49):18450–18457, 2006. doi: 10.1073/pnas.0605697103.

J. H. Doelling, J. M. Walker, E. M. Friedman, A. R. Thompson, and R. D. Vierstra. The apg8/12-activating enzyme apg7 is required for proper nutrient recycling and senescence in arabidopsis thaliana. *The Journal of biological chemistry*, 277(36):33105–33114, 2002. ISSN 0021-9258. doi: 10.1074/jbc.M204630200.

N. Dunken, L. Mahdi, R. E. Häusler, and A. Zuccaro. Monitoring cell death via ion leakage and pam fluorometry. *Plant Proteases and Plant Cell Death: Methods and Protocols*, pages 175–183, 2022. doi: 10.1007/978-1-0716-2079-3_14.

N. Dunken, H. Widmer, G. U. Balcke, H. Straube, G. Langen, N. M. Charura, P. Saake, C. de Quattro, J. Schön, H. Rövenich, S. Wawra, A. Djamei, M. D. Zurbriggen, A. Tissier, C.-P. Witte, and A. Zuccaro. A nucleoside signal generated by a fungal endophyte regulates host cell death and promotes root colonization. *bioRxiv*, 2023. doi: 10.1101/2022.03.11.483938. URL `https://www.biorxiv.org/content/early/2023/02/01/2022.03.11.483938`.

G. Estrada-Navarrete, N. Cruz-Mireles, R. Lascano, X. Alvarado-Affantranger, A. Hernández-Barrera, A. Barraza, J. E. Olivares, M.-K. Arthikala, L. Cárdenas, C. Quinto, and F. Sanchez. An autophagy-related kinase is essential for the symbiotic relationship between phaseolus vulgaris and both rhizobia and arbuscular mycorrhizal fungi. *The Plant cell*, 28(9):2326–2341, 2016. doi: 10.1105/tpc.15.01012.

D. R. Green, L. Galluzzi, and G. Kroemer. Cell biology. metabolic control of cell death. *Science*, 345(6203):1250256, 2014. doi: 10.1126/science.1250256.

T. Hackenberg, T. Juul, A. Auzina, S. Gwizdz, A. Malolepszy, K. van der Kelen, S. Dam, S. Bressendorff, A. Lorentzen, P. Roepstorff, K. Lehmann Nielsen, J.-E. Jørgensen, D. Hofius, F. van Breusegem, M. Petersen, and S. U. Andersen. Catalase and no catalase activity1 promote autophagy-dependent cell death in arabidopsis. *The Plant cell*, 25(11):4616–4626, 2013. doi: 10.1105/tpc.113.117192.

S. Han, Y. Wang, X. Zheng, Q. Jia, J. Zhao, F. Bai, Y. Hong, and Y. Liu. Cytoplastic glyceraldehyde-3-phosphate dehydrogenases interact with atg3 to negatively regulate autophagy and immunity in nicotiana benthamiana. *The Plant cell*, 27(4):1316–1331, 2015. doi: 10.1105/tpc.114.134692.

H. Hanaoka, T. Noda, Y. Shirano, T. Kato, H. Hayashi, D. Shibata, S. Tabata, and Y. Ohsumi. Leaf senescence and starvation-induced chlorosis are accelerated by the disruption of an arabidopsis autophagy gene. *Plant physiology*, 129(3):1181–1193, 2002. ISSN 0032-0889. doi: 10.1104/pp.011024.

M. Havé, J. Luo, F. Tellier, T. Balliau, G. Cueff, F. Chardon, M. Zivy, L. Rajjou, J.-L. Cacas, and C. Masclaux-Daubresse. Proteomic and lipidomic analyses of the arabidopsis atg5 autophagy mutant reveal major changes in endoplasmic reticulum and peroxisome metabolisms and in lipid composition. *The New phytologist*, 223(3):1461–1477, 2019. doi: 10.1111/nph.15913.

A. P. Hayward, J. Tsao, and S. P. Dinesh-Kumar. Autophagy and plant innate immunity: Defense through degradation. *Seminars in cell & developmental biology*, 20(9):1041–1047, 2009. doi: 10.1016/j.semcdb.2009.04.012.

C. He and D. J. Klionsky. Regulation mechanisms and signaling pathways of autophagy. *Annual review of genetics*, 43:67–93, 2009. doi: 10.1146/annurev-genet-102808-114910.

Y. He, H. Fukushige, D. F. Hildebrand, and S. Gan. Evidence supporting a role of jasmonic acid in arabidopsis leaf senescence. *Plant physiology*, 128(3):876–884, 2002. ISSN 0032-0889. doi: 10.1104/pp.010843.

M. Hilbert, L. M. Voll, Y. Ding, J. Hofmann, M. Sharma, and A. Zuccaro. Indole derivative production by the root endophyte piriformospora indica is not required for growth promotion but for biotrophic colonization of barley roots. *The New phytologist*, 196(2):520–534, 2012. doi: 10.1111/j.1469-8137.2012.04275.x.

D. Hofius, T. Schultz-Larsen, J. Joensen, D. I. Tsitsigiannis, N. H. T. Petersen, O. Mattsson, L. B. Jørgensen, J. D. G. Jones, J. Mundy, and M. Petersen. Autophagic components contribute to hypersensitive cell death in arabidopsis. *Cell*, 137(4):773–783, 2009. doi: 10.1016/j.cell.2009.02.036.

D. Hofius, L. Li, A. Hafrén, and N. S. Coll. Autophagy as an emerging arena for plant-pathogen interactions. *Current opinion in plant biology*, 38:117–123, 2017. doi: 10.1016/j.pbi.2017.04.017.

G. Hoxhaj, J. Hughes-Hallett, R. C. Timson, E. Ilagan, M. Yuan, J. M. Asara, I. Ben-Sahra, and B. D. Manning. The mtorc1 signaling network senses changes in cellular purine nucleotide levels. *Cell reports*, 21(5):1331–1346, 2017. doi: 10.1016/j.celrep.2017.10.029.

S. Jacobs, B. Zechmann, A. Molitor, M. Trujillo, E. Petutschnig, V. Lipka, K.-H. Kogel, and P. Schäfer. Broad-spectrum suppression of innate immunity is required for colonization of arabidopsis roots by the fungus piriformospora indica. *Plant physiology*, 156(2):726–740, 2011. ISSN 0032-0889. doi: 10.1104/pp.111.176446.

J. D. G. Jones and J. L. Dangl. The plant immune system. *Nature*, 444(7117):323–329, 2006. doi: 10.1038/nature05286.

A. Katsiarimpa, K. Kalinowska, F. Anzenberger, C. Weis, M. Ostertag, C. Tsutsumi, C. Schwechheimer, F. Brunner, R. Hückelhoven, and E. Isono. The deubiquitinating enzyme amsh1 and the escrt-iii subunit vps2.1 are required for autophagic degradation in arabidopsis. *The Plant cell*, 25(6):2236–2252, 2013. doi: 10.1105/tpc.113.113399.

Z. Kazibwe, J. Soto-Burgos, G. C. MacIntosh, and D. C. Bassham. Tor mediates the autophagy response to altered nucleotide homeostasis in an rnase mutant. *Journal of experimental botany*, 71 (22):6907–6920, 2020. doi: 10.1093/jxb/eraa410.

D. Kim, B. Langmead, and S. L. Salzberg. Hisat: a fast spliced aligner with low memory requirements. *Nature methods*, 12(4):357–360, 2015. doi: 10.1038/nmeth.3317.

D. J. Klionsky, A. K. Abdel-Aziz, S. Abdelfatah, M. Abdellatif, A. Abdoli, S. Abel, and et al. Guidelines for the use and interpretation of assays for monitoring autophagy (4th edition). *Autophagy*, 17(1):1–382, 2021. doi: 10.1080/15548627.2020.1797280.

U. Lahrmann and A. Zuccaro. Opprimo ergo sum–evasion and suppression in the root endophytic fungus piriformospora indica. *Molecular plant-microbe interactions : MPMI*, 25(6):727–737, 2012. ISSN 0894-0282. doi: 10.1094/MPMI-11-11-0291.

U. Lahrmann, Y. Ding, A. Banhara, M. Rath, M. R. Hajirezaei, S. Döhlemann, N. von Wirén, M. Parniske, and A. Zuccaro. Host-related metabolic cues affect colonization strategies of a root endophyte. *Proceedings of the National Academy of Sciences*, 110(34):13965–13970, 2013. doi: 10.1073/pnas.1301653110.

U. Lahrmann, N. Strehmel, G. Langen, H. Frerigmann, L. Leson, Y. Ding, D. Scheel, S. Herklotz, M. Hilbert, and A. Zuccaro. Mutualistic root endophytism is not associated with the reduction of saprotrophic traits and requires a noncompromised plant innate immunity. *The New phytologist*, 207(3):841–857, 2015. doi: 10.1111/nph.13411.

Z. Lai, F. Wang, Z. Zheng, B. Fan, and Z. Chen. A critical role of autophagy in plant resistance to necrotrophic fungal pathogens. *The Plant Journal*, 66(6):953–968, 2011. ISSN 0960-7412. doi: 10.1111/j.1365-313X.2011.04553.x.

A. Y. Leary, Z. Savage, Y. Tumtas, and T. O. Bozkurt. Contrasting and emerging roles of autophagy in plant immunity. *Current opinion in plant biology*, 52:46–53, 2019. doi: 10.1016/j.pbi.2019.07.002.

H. D. Lenz, E. Haller, E. Melzer, K. Kober, K. Wurster, M. Stahl, D. C. Bassham, R. D. Vierstra, J. E. Parker, J. Bautor, A. Molina, V. Escudero, T. Shindo, R. A. L. van der Hoorn, A. A. Gust, and T. Nürnberger. Autophagy differentially controls plant basal immunity to biotrophic and necrotrophic pathogens. *The Plant Journal*, 66(5):818–830, 2011. ISSN 0960-7412. doi: 10.1111/j.1365-313X.2011.04546.x.

F. Li, T. Chung, J. G. Pennington, M. L. Federico, H. F. Kaeppler, S. M. Kaeppler, M. S. Otegui, and R. D. Vierstra. Autophagic recycling plays a central role in maize nitrogen remobilization. *The Plant cell*, 27(5):1389–1408, 2015. doi: 10.1105/tpc.15.00158.

G. Li, K. Liu, S. A. Baldwin, and D. Wang. Equilibrative nucleoside transporters of arabidopsis thaliana. cdna cloning, expression pattern, and analysis of transport activities. *The Journal of biological chemistry*, 278(37):35732–35742, 2003. ISSN 0021-9258. doi: 10.1074/jbc.M304768200.

Y. Liao, G. K. Smyth, and W. Shi. featurecounts: an efficient general purpose program for assigning sequence reads to genomic features. *Bioinformatics*, 30(7):923–930, 2014. ISSN 1367-4803. doi: 10.1093/bioinformatics/btt656.

Y. Liu and D. C. Bassham. Autophagy: pathways for self-eating in plant cells. *Annual review of plant biology*, 63:215–237, 2012. doi: 10.1146/annurev-arplant-042811-105441.

L. Lo Presti, D. Lanver, G. Schweizer, S. Tanaka, L. Liang, M. Tollot, A. Zuccaro, S. Reissmann, and R. Kahmann. Fungal effectors and plant susceptibility. *Annual review of plant biology*, 66: 513–545, 2015. doi: 10.1146/annurev-arplant-043014-114623.

M. I. Love, W. Huber, and S. Anders. Moderated estimation of fold change and dispersion for rna-seq data with deseq2. *Genome biology*, 15(12):550, 2014. doi: 10.1186/s13059-014-0550-8.

R. S. Marshall and R. D. Vierstra. Autophagy: The master of bulk and selective recycling. *Annual review of plant biology*, 69:173–208, 2018. doi: 10.1146/annurev-arplant-042817-040606.

R. S. Marshall, F. Li, D. C. Gemperline, A. J. Book, and R. D. Vierstra. Autophagic degradation of the 26s proteasome is mediated by the dual atg8/ubiquitin receptor rpn10 in arabidopsis. *Molecular cell*, 58(6):1053–1066, 2015. doi: 10.1016/j.molcel.2015.04.023.

N. Mizushima, T. Yoshimori, and Y. Ohsumi. The role of atg proteins in autophagosome formation. *Annual review of cell and developmental biology*, 27:107–132, 2011. doi: 10.1146/annurev-cellbio-092910-154005.

D. Munch, E. Rodriguez, S. Bressendorff, O. K. Park, D. Hofius, and M. Petersen. Autophagy deficiency leads to accumulation of ubiquitinated proteins, er stress, and cell death in arabidopsis. *Autophagy*, 10(9):1579–1587, 2014. doi: 10.4161/auto.29406.

D. Munch, O.-K. Teh, F. G. Malinovsky, Q. Liu, R. R. Vetukuri, F. El Kasmi, P. Brodersen, I. Hara-Nishimura, J. L. Dangl, M. Petersen, J. Mundy, and D. Hofius. Retromer contributes to immunity-associated cell death in arabidopsis. *The Plant cell*, 27(2):463–479, 2015. doi: 10.1105/tpc.114.132043.

S. Nizam, X. Qiang, S. Wawra, R. Nostadt, F. Getzke, F. Schwanke, I. Dreyer, G. Langen, and A. Zuccaro. Serendipita indica e5'nt modulates extracellular nucleotide levels in the plant apoplast and affects fungal colonization. *EMBO reports*, 20(2), 2019. doi: 10.15252/embr.201847430.

F. Oberwinkler, K. Riess, R. Bauer, M.-A. Selosse, M. Weiß, S. Garnica, and A. Zuccaro. Enigmatic sebacinales. *Mycological Progress*, 12(1):1–27, 2013. ISSN 1617-416X. doi: 10.1007/s11557-012-0880-4.

Y. Olvera-Carrillo, M. van Bel, T. van Hautegem, M. Fendrych, M. Huysmans, M. Simaskova, M. van Durme, P. Buscaill, S. Rivas, N. S. Coll, F. Coppens, S. Maere, and M. K. Nowack. A conserved core of programmed cell death indicator genes discriminates developmentally and environmentally induced programmed cell death in plants. *Plant physiology*, 169(4):2684–2699, 2015. ISSN 0032-0889. doi: 10.1104/pp.15.00769.

P. Pandey, A. Y. Leary, Y. Tumtas, Z. Savage, B. Dagvadorj, C. Duggan, E. L. Yuen, N. Sanguankiattichai, E. Tan, V. Khandare, A. J. Connerton, T. Yunusov, M. Madalinski, F. G. Mirkin, S. Schornack, Y. Dagdas, S. Kamoun, and T. O. Bozkurt. An oomycete effector subverts host vesicle trafficking to channel starvation-induced autophagy to the pathogen interface. *eLife*, 10, 2021. doi: 10.7554/eLife.65285.

A. R. Phillips, A. Suttangkakul, and R. D. Vierstra. The atg12-conjugating enzyme atg10 is essential for autophagic vesicle formation in arabidopsis thaliana. *Genetics*, 178(3):1339–1353, 2008. ISSN 0016-6731. doi: 10.1534/genetics.107.086199.

X. Qiang, B. Zechmann, M. U. Reitz, K.-H. Kogel, and P. Schäfer. The mutualistic fungus piriformospora indica colonizes arabidopsis roots by inducing an endoplasmic reticulum stress-triggered caspase-dependent cell death. *The Plant cell*, 24(2):794–809, 2012. doi: 10.1105/tpc.111.093260.

M. Raffeiner, S. Zhu, M. González-Fuente, and S. Üstün. Interplay between autophagy and proteasome during protein turnover. *Trends in plant science*, 28(6):698–714, 2023. doi: 10.1016/j.tplants.2023.01.013.

P. Schäfer, S. Pfiffi, L. M. Voll, D. Zajic, P. M. Chandler, F. Waller, U. Scholz, J. Pons-Kühnemann, S. Sonnewald, U. Sonnewald, and K.-H. Kogel. Manipulation of plant innate immunity and gibberellin as factor of compatibility in the mutualistic association of barley roots with piriformospora indica. *The Plant Journal*, 59(3):461–474, 2009. ISSN 0960-7412. doi: 10.1111/j.1365-313X.2009.03887.x.

J. Schippers, H.-C. Jing, J. Hille, and P. Dijkwel. Developmental and hormonal control of leaf senescence. *Senescence Processes in Plants*, 2007. ISSN 97814051. doi: 10.1002/9780470988855.ch7.

M. Stephani, L. Picchianti, A. Gajic, R. Beveridge, E. Skarwan, V. Sanchez de Medina Hernandez, A. Mohseni, M. Clavel, Y. Zeng, C. Naumann, M. Matuszkiewicz, E. Turco, C. Loefke, B. Li, G. Dürnberger, M. Schutzbier, H. T. Chen, A. Abdrakhmanov, A. Savova, K.-S. Chia, A. Djamei, I. Schaffner, S. Abel, L. Jiang, K. Mechtler, F. Ikeda, S. Martens, T. Clausen, and Y. Dagdas. A cross-kingdom conserved er-phagy receptor maintains endoplasmic reticulum homeostasis during stress. *eLife*, 9, 2020. doi: 10.7554/eLife.58396.

V. Thammavongsa, D. M. Missiakas, and O. Schneewind. Staphylococcus aureus degrades neutrophil extracellular traps to promote immune cell death. *Science*, 342(6160):863–866, 2013. doi: 10.1126/science.1242255.

A. R. Thompson, J. H. Doelling, A. Suttangkakul, and R. D. Vierstra. Autophagic nutrient recycling in arabidopsis directed by the atg8 and atg12 conjugation pathways. *Plant physiology*, 138(4): 2097–2110, 2005. ISSN 0032-0889. doi: 10.1104/pp.105.060673.

J. Thürich, D. Meichsner, A. C. U. Furch, J. Pfalz, T. Krüger, O. Kniemeyer, A. Brakhage, and R. Oelmüller. Arabidopsis thaliana responds to colonisation of piriformospora indica by secretion of symbiosis-specific proteins. *PloS one*, 13(12):e0209658, 2018. doi: 10.1371/journal.pone.0209658.

S. Üstün, A. Hafrén, and D. Hofius. Autophagy as a mediator of life and death in plants. *Current opinion in plant biology*, 40:122–130, 2017. doi: 10.1016/j.pbi.2017.08.011.

S. Wada, H. Ishida, M. Izumi, K. Yoshimoto, Y. Ohsumi, T. Mae, and A. Makino. Autophagy plays a role in chloroplast degradation during senescence in individually darkened leaves. *Plant physiology*, 149(2):885–893, 2009. ISSN 0032-0889. doi: 10.1104/pp.108.130013.

F. Waller, B. Achatz, H. Baltruschat, J. Fodor, K. Becker, M. Fischer, T. Heier, R. Hückelhoven, C. Neumann, D. von Wettstein, P. Franken, and K.-H. Kogel. The endophytic fungus piriformospora indica reprograms barley to salt-stress tolerance, disease resistance, and higher yield. *Proceedings of the National Academy of Sciences*, 102(38):13386–13391, 2005. doi: 10.1073/pnas.0504423102.

Y. Wang, M. T. Nishimura, T. Zhao, and D. Tang. Atg2, an autophagy-related protein, negatively affects powdery mildew resistance and mildew-induced cell death in arabidopsis. *The Plant Journal*, 68(1):74–87, 2011. ISSN 0960-7412. doi: 10.1111/j.1365-313X.2011.04669.x.

M. Weiß, F. Waller, A. Zuccaro, and M.-A. Selosse. Sebacinales - one thousand and one interactions with land plants. *The New phytologist*, 211(1):20–40, 2016. doi: 10.1111/nph.13977.

V. Winstel, D. Missiakas, and O. Schneewind. Staphylococcus aureus targets the purine salvage pathway to kill phagocytes. *Proceedings of the National Academy of Sciences*, 115(26):6846–6851, 2018. doi: 10.1073/pnas.1805622115.

Y. Xiong, A. L. Contento, P. Q. Nguyen, and D. C. Bassham. Degradation of oxidized proteins by autophagy during oxidative stress in arabidopsis. *Plant physiology*, 143(1):291–299, 2007. ISSN 0032-0889. doi: 10.1104/pp.106.092106.

K. Yoshimoto, H. Hanaoka, S. Sato, T. Kato, S. Tabata, T. Noda, and Y. Ohsumi. Processing of atg8s, ubiquitin-like proteins, and their deconjugation by atg4s are essential for plant autophagy. *The Plant cell*, 16(11):2967–2983, 2004. doi: 10.1105/tpc.104.025395.

K. Yoshimoto, Y. Jikumaru, Y. Kamiya, M. Kusano, C. Consonni, R. Panstruga, Y. Ohsumi, and K. Shirasu. Autophagy negatively regulates cell death by controlling npr1-dependent salicylic acid signaling during senescence and the innate immune response in arabidopsis. *The Plant cell*, 21(9):2914–2927, 2009. doi: 10.1105/tpc.109.068635.

A. Zuccaro, U. Lahrmann, U. Güldener, G. Langen, S. Pfiffi, D. Biedenkopf, P. Wong, B. Samans, C. Grimm, M. Basiewicz, C. Murat, F. Martin, and K.-H. Kogel. Endophytic life strategies decoded by genome and transcriptome analyses of the mutualistic root symbiont piriformospora indica. *PLoS pathogens*, 7(10):e1002290, 2011. doi: 10.1371/journal.ppat.1002290.

Figures and descriptions

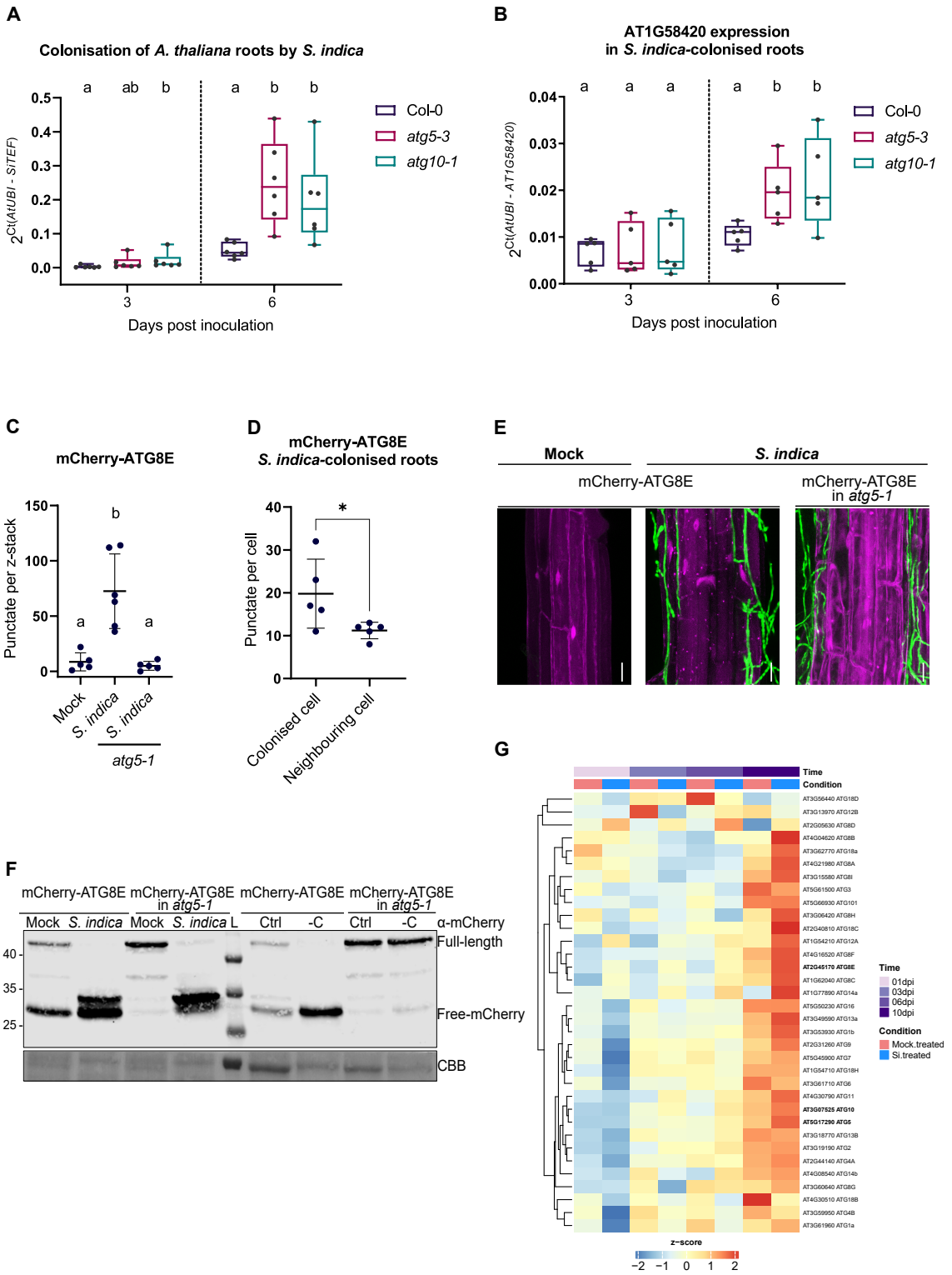

Figure 1: Involvement of autophagy in the colonisation of *A. thaliana* roots by *S. indica*. (**A**) *S. indica* colonisation of Col-0 and autophagy mutants *atg5-3* and *atg10-1* quantified by RT-qPCR at 3 and 6 days post inoculation (dpi). Fungal colonisation in plant root tissue was calculated from the ratio of *S. indica* (*SiTEF*) to plant (*AtUbi*) using cDNA as template and the $2^{-\Delta C_t}$ method. Boxplots with whiskers extending to the minimum and maximum values represent data from 6 independent biological replicates. Different letters indicate significant differences ($p < 0.05$) according to Kruskal-Wallis test and post-hoc Dunn test using Benjamini-Hochberg for false discovery rate correction. (**B**) Expression of the marker gene AT1G58420 in *S. indica*-colonised Col-0, *atg5-3* and *atg10-1* roots at 6 dpi. Relative expression was calculated compared to plant (*AtUbi*) using cDNA as template and the $2^{-\Delta C_t}$ method. Boxplots with whiskers extending to the minimum and maximum values represent data from 5 independent biological replicates. Different letters indicate significant differences ($p < 0.05$) according to Kruskal-Wallis test and post-hoc Dunn test using Benjamini-Hochberg for false discovery rate correction. (**C**) Quantification of mCherry-ATG8E-labeled puncta was performed using confocal images of transgenic roots expressing mCherry-ATG8E. Confocal microscopy was conducted on differentiated root cells following mock or *S. indica* inoculation. The scatter plot (mean $\pm$ SD) shows the total number of puncta per z-stack in the whole 63X captured image for mCherry-ATG8E mock (n=5), *S. indica* (n=6), and mCherry-ATG8E in *atg5-1 S. indica* (n=5). The images represent maximal projections of 8-10 optical sections. Different letters indicate significant differences ($p < 0.05$) according to one-way ANOVA with post-hoc Tukey HSD test. (**D**) Quantification of mCherry-ATG8E-labeled puncta was performed using confocal images of transgenic roots expressing mCherry-ATG8E. Confocal microscopy was conducted on differentiated root cells colonised by *S. indica*. The scatter plot (mean $\pm$ SD) shows the number of mCherry-ATG8 puncta per root cell distinguishing between cells with hyphal contact and neighbouring cells without hyphal contact (n=5). The images represent maximal projections of 8-10 optical sections. The asterisk indicates significant differences ($p < 0.05$) according to unpaired Student's t-test. (**E**) Confocal laser scanning microscopy (CLSM) images were obtained of transgenic roots expressing mCherry-ATG8E in WT or *atg5-1* background. The microscopy was conducted from the epidermis of differentiated root cells, following mock or *S. indica* treatment for 10 days after seed inoculation. The images represent maximal projections of 8-10 optical sections, scale bar 20 µm. (**F**) Autophagy flux analysis was performed using transgenic plants expressing mCherry-ATG8E in WT or *atg5-1* background. The left panel displays a blot with samples obtained from collected roots upon mock or *S. indica* treatment for 10 days after seed inoculation. The right panel displays a blot with samples obtained from collected seedlings incubated in control or carbon-depleted media for starvation-induced autophagy. Immunoblot analysis was performed using an anti-mCherry antibody. Coomassie Brilliant Blue (CBB) was used as protein loading control. (**G**) Heatmap with expression levels of autophagy-related genes (ATG) from Arabidopsis WT roots samples collected at 1, 3, 6 and 10 days post inoculation with mock or *S. indica* (Si). Genes with an average TPM value > 1 TPM across all samples were selected. The heatmap shows the z-score of log2 transformed TPM + 1 values of selected Arabidopsis genes. For each condition the average expression across the three biological replicates is represented. The full version of the heatmap of autophagy-associated genes can be found in Figure S2.

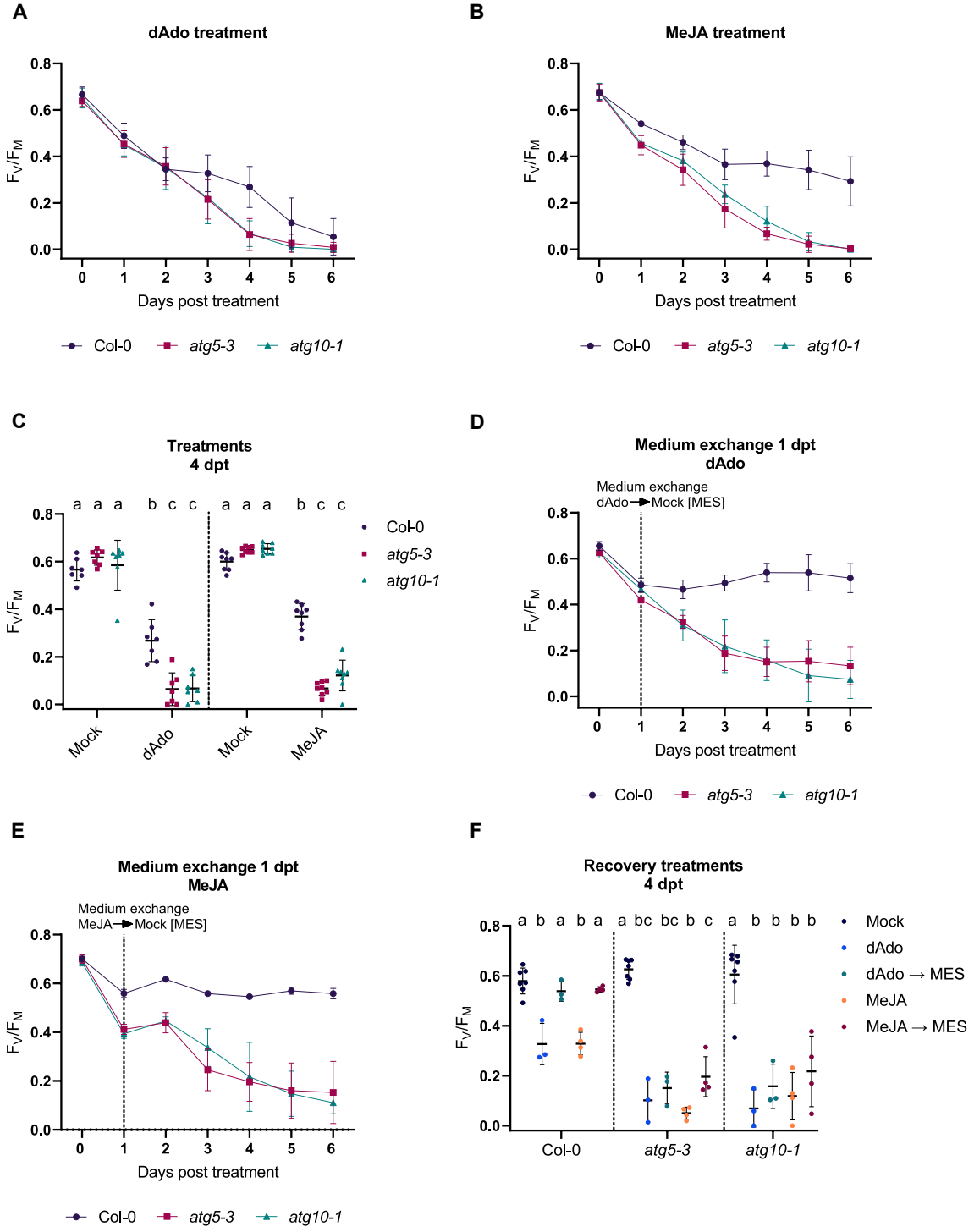
A
dAdo treatment
B
MeJA treatment
C
Treatments
4 dpt
D
Medium exchange 1 dpt
dAdo
Medium exchange
dAdo → Mock [MES]
E
Medium exchange 1 dpt
MeJA
Medium exchange
MeJA → Mock [MES]
F
Recovery treatments
4 dpt
F_V/F_M
Days post treatment
Col-0
atg5-3
atg10-1
Mock
dAdo
MeJA
dAdo → MES
MeJA → MES

Figure 2: Autophagy promotes cell survival during dAdo-induced cell death.
(**A**) Photosystem II maximum quantum yield (F_V/F_M) of nine-day-old seedlings treated with mock (MES 2.5 mM buffer) or dAdo (500 µM), measured by PAM fluorometry. Error bars represent ± SD of the mean of 7 independent biological replicates. (**B**) Photosystem II maximum quantum yield (F_V/F_M) of nine-day-old seedlings treated with mock (MES 2.5 mM buffer) or methyl jasmonate (MeJA, 500 µM) as positive control for senescence-induced cell death, measured by PAM fluorometry. Error bars represent ± SD of the mean of 8 independent biological replicates. (**C**) Quantification of (F_v/F_m) of Col-0 and autophagy mutants *atg5-3* and *atg10-1*, 4 days post treatment (dpt). The scatter plot (mean ± SD) represents data from 7-8 independent biological replicates with 12 technical replicates each. Different letters indicate significant differences ($p < 0.05$) according to one-way ANOVA with post-hoc Tukey HSD test. (**D**) Photosystem II maximum quantum yield (F_V/F_M) of nine-day-old seedlings treated with mock (MES 2.5 mM buffer) or dAdo (500 µM), measured by PAM fluorometry. dAdo treatment solution was replaced after 24 h with MES 2.5 mM buffer. Error bars represent ± SD of the mean of 3 independent biological replicates (**E**) Photosystem II maximum quantum yield (F_V/F_M) of nine-day-old seedlings treated with mock (MES 2.5 mM buffer) or methyl jasmonate (MeJA, 500 µM), measured by PAM fluorometry. MeJA treatment solution was replaced after 24 h with MES 2.5 mM buffer. Error bars represent ± SD of the mean of 4 independent biological replicates. (**F**) Quantification of (F_V/F_M) of Col-0 and autophagy mutants *atg5-3* and *atg10-1*, 4 days after treatment solution replacement. The scatter plot (mean ± SD) represents data from 3-4 independent biological replicates with 12 technical replicates each. Different letters indicate significant differences ($p < 0.05$) according to one-way ANOVA with post-hoc Tukey HSD test.

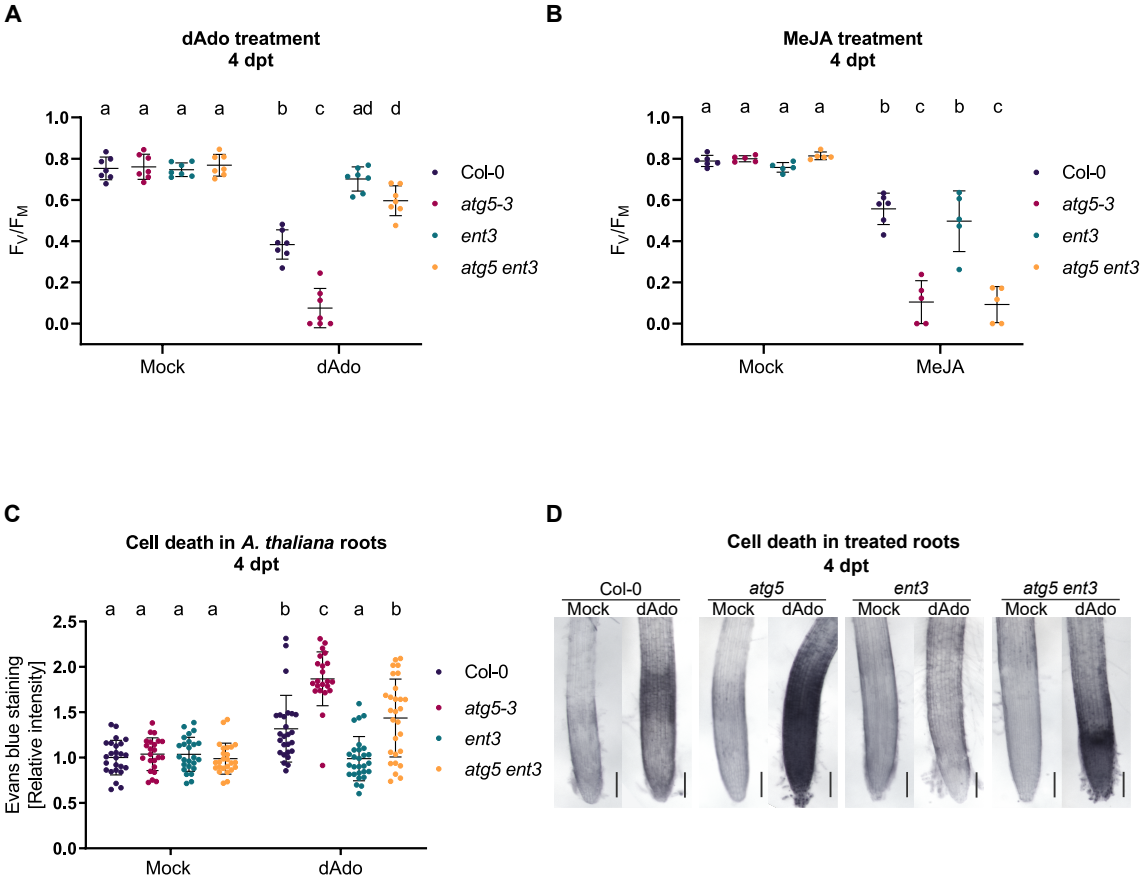

Figure 3: The double mutant *atg5 ent3* displays a dAdo resistance phenotype. (**A**) Quantification of photosystem II maximum quantum yield (F_V/F_M) of Col-0, *atg5-3*, *ent3* and *atg5 ent3* at 4 days post treatment (dpt) by PAM fluorometry. Nine-day-old seedlings were treated with mock (MES 2.5 mM buffer) or dAdo (500 µM). The scatter plot (mean ± SD) represents data from 7 independent biological replicates with 12 technical replicates each. Different letters indicate significant differences ($p < 0.05$) according to one-way ANOVA with post-hoc Tukey HSD test. (**B**) Quantification of photosystem II maximum quantum yield (F_V/F_M) of Col-0, *atg5-3*, *ent3* and *atg5 ent3* at 4 dpt by PAM fluorometry. Nine-day-old seedlings were treated with mock (MES 2.5 mM buffer) or methyl jasmonate (MeJA, 500 µM). The scatter plot (mean ± SD) represents data from 5 independent biological replicates with 12 technical replicates each. Different letters indicate significant differences ($p < 0.05$) according to one-way ANOVA with post-hoc Tukey HSD test. (**C**) Quantification of cell death at the root tip of Col-0, *atg5-3*, *ent3* and *atg5 ent3*. Eight-day-old seedlings were treated with mock (sterile milli-Q water) or dAdo (500 µM) and stained with Evans blue after 4 dpt. The scatter plot (mean ± SD) represents relative values to Col-0 mock from 22-28 biological replicates. Different letters indicate significant differences ($p < 0.05$) according to Kruskal-Wallis test and post-hoc Dunn test using Benjamini-Hochberg for false discovery rate correction. (**D**) Bright-field microscopy of root cell death at the root tip in Col-0, *atg5-3*, *ent3* and *atg5 ent3* seedlings incubated with mock or dAdo (500 µM) and stained with Evans blue dye 4 days after treatment. Scale bar 500 µm.

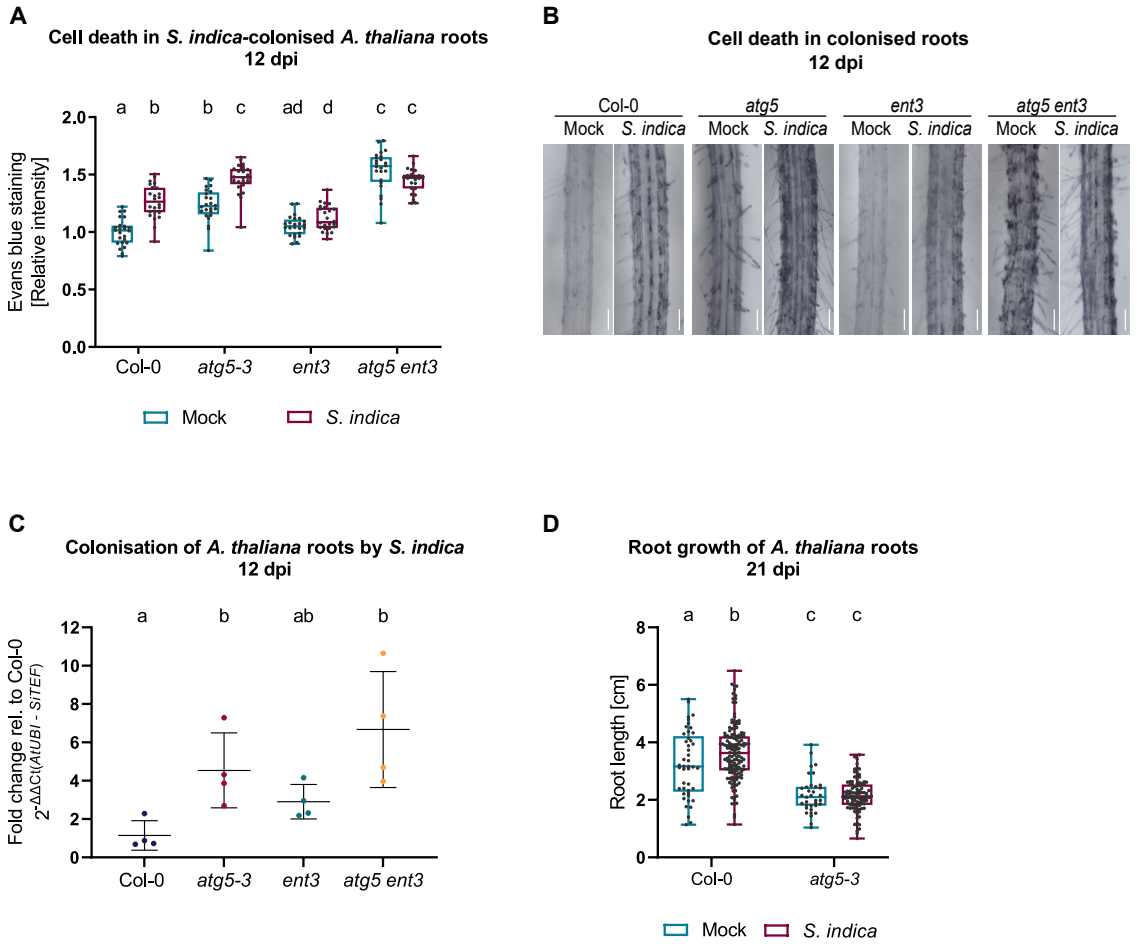

Figure 4: The double mutant *atg5 ent3* precludes *S. indica*-mediated cell death. (**A**) Quantification of cell death at the root differentiation zone in Col-0, *atg5-3*, *ent3* and *atg5 ent3*. Seedlings were inoculated with mock or *S. indica* and stained with Evans Blue dye after 12 post inoculation (dpi). Boxplots with whiskers extending to the minimum and maximum values represent relative values to Col-0 mock from 6 independent biological replicates. Different letters indicate significant differences ($p < 0.05$) according to Kruskal-Wallis test and post-hoc Dunn test using Benjamini-Hochberg for false discovery rate correction. (**B**) Bright-field microscopy of root cell death at the differentiation zone in Col-0, *atg5-3*, *ent3* and *atg5 ent3* seedlings inoculated with mock or *S. indica* and stained with Evans blue dye at 12 dpi. Scale bar 500 µm. (**C**) *S. indica* colonisation of Col-0, *atg5-3*, *ent3* and *atg5 ent3* quantified by RT-qPCR at 12 dpi. Fungal colonisation in plant root tissue was calculated from the ratio of *S. indica* (*SiTEF*) to plant (*AtUbi*) using cDNA as template and the $2^{-\Delta\Delta C_t}$ method. The scatter plot (mean ± SD) represents relative values to Col-0 from 4 independent biological replicates. Different letters indicate significant differences ($p < 0.05$) according to Kruskal-Wallis test and post-hoc Dunn test using Benjamini-Hochberg for false discovery rate correction. (**D**) Root length of Col-0 and *atg5-3* seedlings after 21 days under mock or *S. indica* treatment. Boxplots with whiskers extending to the minimum and maximum values represent data from 5-12 independent biological replicates with each 20 roots. Different letters indicate significant differences ($p < 0.05$) according to Kruskal-Wallis test and post-hoc Dunn test using Benjamini-Hochberg for false discovery rate correction.

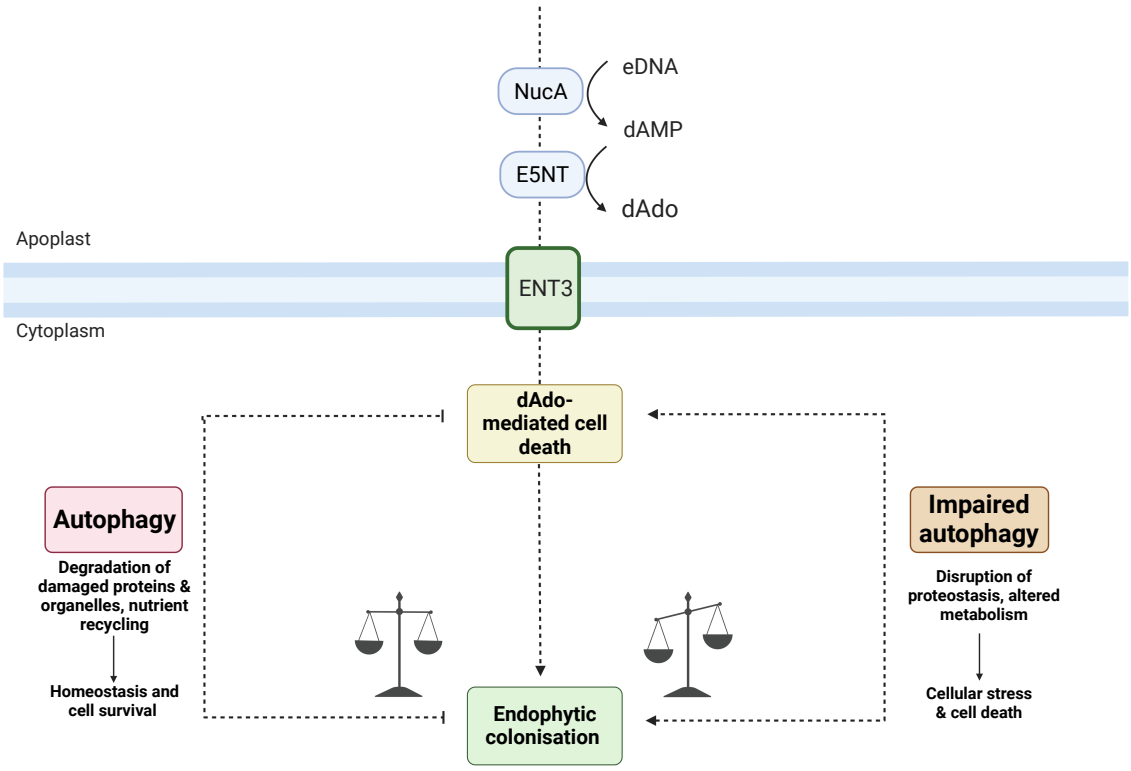

Figure 5: Current model for the crosstalk between autophagy and dAdo cell death during *S. indica* colonisation.
Endophytic root colonisation of the host plant *Arabidopsis thaliana* by the beneficial root endophyte *Serendipita indica* (*S. indica*) is characterised by a biotrophic phase followed by a restricted cell-death associated phase. The activity of two secreted effector enzymes of *S. indica*, E5NT and NucA, produces a DNA-derived deoxynucleoside called deoxyadenosine (dAdo) (Dunken et al., 2023). Extracellular dAdo is imported into the cytoplasm by the Arabidopsis equilibrative nucleoside transporter ENT3, activating a dAdo-dependent regulated cell death. Autophagy, a major degradation and nutrient recycling pathway that maintains cellular homeostasis and modulates metabolism, plays a key role in the beneficial interaction between *S. indica* and Arabidopsis. Autophagy restricts fungal colonisation and provides a protective function against dAdo-induced cell death. We propose that autophagy-driven pro-survival responses, such as the degradation of damaged proteins or protein aggregates and the recycling of nutrients, facilitate a balanced symbiotic interaction. Illustration was designed using Biorender online tool.